Journal of
Ceramic Science
and Technology

J. Ceram. Sci. Technol., **12** [1] 37-48 (2021)
DOI: 10.4416/JCST2021-00005
available online at: http://www.ceramic-science.com

Fabrication of complicated silicon carbide ceramic components by acrylate gel-casting

Chuanru Cao, Shuyue Gao, Ying Sun, Bohang Xing*, Cao Wang*, Zhe Zhao*

School of Materials Science and Engineering, Shanghai Institute of Technology, Shanghai 201418, China
received March 16, 2021; received in revised form March 22, 2021; accepted March 23, 2021

Abstract

Solid-state sintered silicon carbide (SiC) ceramics with respectable performance were successfully prepared with a gel casting method. Only acrylic resins were used as dispersants to form a thermally gellable SiC ceramic slurry with reasonable solid load of 45 vol%. The effect of the dispersants and solid load on the stability and rheological behaviour of the SiC suspensions has been systematically discussed. It has been established that the sintering performance, microstructure and mechanical properties of SiC ceramics are significantly affected by the rheology behaviour of the SiC suspensions. Finally, sintered samples with a relative density of 95.16 % (3.05 g/cm^3) and a flexural strength of 377.4 MPa were achieved with the gel casting method.

Keywords: Gel casting, SiC, rheological behaviour, complex structural, mechanical properties

I. Introduction

Because of their excellent mechanical, chemical, oxidation and thermal properties [1–3], silicon carbide (SiC) ceramics have been widely applied in the aerospace [4], nuclear [5] and rail transportation industries [6]. Various traditional forming techniques, such as dry pressing [7], cold isostatic pressing [8], slip casting [9], injection moulding [10] and tape casting [11], have been successfully used to prepare SiC ceramics. However, the high hardness and brittleness of silicon carbide ceramics make it difficult to realize complex-shaped SiC parts with excellent mechanical properties. Recently, with the development of different three-dimensional (3D) printing methods, it has become possible to resolve this fundamental problem. Some additive manufacturing techniques have been studied for the fabrication of SiC ceramics, such as direct ink writing [12], selective laser sintering [13] and stereolithography [14]. Compton *et al.* [12] fabricated SiC/C filled ceramics using a extrusion 3D printing method; the relative density and flexural strength of the sintered samples measured 50.9 % and 96.3 MPa, respectively. Larson *et al.* [15] prepared 3D SiC structures by means of direct ink writing technology with a relative density of 48.9 % and a flexural strength of 70.4 MPa. But reported densities and strength are still low, and it remains difficult to prepare silicon carbide ceramics with high precision on account of the low precision of the direct ink writing technology. Jin *et al.* [13] prepared complex ceramic parts by means of selective laser sintering (SLS) combined with cold isostatic pressing (CIP) and polymer infiltration pyrolysis (PIP). The obtained specimens exhibited a flexural strength of 201 MPa. Liu *et al.* [16] used cold isostatic pressing (CIP) and reactive sintering (RS) techniques to increase the density of SLS-printed complex SiC ceramic materials. The bending strength and density of the final sintered samples were 292 ~ 348 MPa and 2.94 ~ 2.98 g/cm^3, respectively. However, laser sintering introduces high temperature gradients, which can easily produce internal stress and cracks, thus reducing the strength of the samples. He *et al.* [14] prepared 3D-structured SiC ceramics with the stereolithography method using polymer precursor, and the strength performance of sintered samples was improved with the help of precursor infiltration prior to pyrolysis. Their flexural strength and relative density were 204.6 MPa and 84.8 %, respectively. Zhang *et al.* [17] prepared photosensitive suspension including carbon fibres (C_f), fabricated C_f preforms by means of DLP technology, and used liquid silicon infiltration to improve their strength, ultimately obtaining a flexural strength of 262.6 MPa. Although precursor infiltration and pyrolysis or liquid silicon infiltration can improve densification, the strength still needs to be improved. Besides, the increase in porosity with more organic matter evaporating in the PIP process makes it difficult to prepare highly dense ceramic materials.

The preparation of complex SiC ceramic components by means of gel casting has also been widely studied. Zhang *et al.* [18] applied aqueous gel casting and pressureless sintering to prepare dense SiC ceramics. The flexural strength can reach 531 ± 38 MPa with relative density up to 98 %. However, ceramic green body made from water-based materials generally requires high-temperature drying for at least 24 hours to remove the water. Compared with traditional processing methods, the existing 3D printing technologies still fall short with regard to the mechanical properties of SiC ceramics. Consequently, attempts have been made by other researchers to combine 3D printing with tradition-

* Corresponding author: zhezhao@kth.se

al shaping techniques to pave the way for improved SiC ceramics with reasonably complex shape. Tu *et al.* [19] combined 3D printing, gel casting and liquid drying to develop a new method for preparing complex ceramic shapes. Chen *et al.* [20] used a combination of SLA and gel casting to prepare complex SiC ceramics, the final relative density of which reached 98.13 %. Water-based slurries are commonly used to prepare complex SiC devices by means of traditional gel casting. However, the use of aqueous SiC powder suspension easily leads to crack and defect formation during the drying process. Moreover, the material undergoes high volume shrinkage, and the possible residual stress linked with this shrinkage is not conducive to improving the material's mechanical properties. Besides, the dispersion stability and rheological behaviour of the SiC suspension system also affect the properties of the sintered body.

In this paper, high-solid-load SiC suspension with low viscosity was developed for gel casting, this can potentially provide support for the viable production of high-performance and -precision SiC complex devices. Acrylic resin was used to form a strong and solid SiC ceramic green body in a thermally induced polymerization process. The problem of the cracking of ceramic samples during curing caused by water-based materials is largely avoided. The structure of SiC ceramic samples can be controlled by using DLP to print the resin mould. The effect of dispersant type, dispersant dose and solid load on the stability and rheological behaviour of SiC suspensions were discussed systematically. Complex SiC honeycomb structures could be successfully prepared with the developed gel casting process.

II. Experimental

(1) Raw materials

SiC and B_4C powders (SiC, purity > 99 %, D_{50} = 0.5 μm, oxygen content < 0.5 wt%, Al: 0.34 wt%, Fe < 0.2 wt%; Ningbo FLK Tech. Co., Ltd., China) were used as the raw materials. Acrylic resins (Zhejiang Jiaxing CeramPlus Tech. Co. Ltd., Zhejiang, China) were used as the major curable monomers system. Dibenzoyl peroxide (BPO, Shanghai Aladdin Biochemical Technology Co., Ltd., China) was used in this study as an initiator. The dispersants used in this work were CPD-03 and CPD-05 (Zhejiang Jiaxing CeramPlus Tech. Ltd., Zhejiang, China).

(2) Suspension preparation

The resin mixture was prepared with three resin monomers (2-hydroxyethyl acrylate, 1,6-hexanediol diacrylate and trimethylolpropane triacrylate) with a weight ratio of 3:4:3, as introduced in a previous study [21]. The effect of the different dispersant types (CPD-03 or CPD-03 + CPD-05 mixture) and various dispersant doses were studied to optimize rheology performance. After the acrylic resins and dispersants had been carefully mixed and stirred, boron carbide powders were added as sintering aids. And then SiC powders were added to the mixture. Finally, SiC powders were mixed into the slurry prior to the addition of the initiator (BPO). To obtain a uniform silicon carbide slurry, the mixture was milled further for 1 h. Based on different types of dispersants (CPD-03 or CPD-03 + CPD-05 mixture), the different proportions of dispersant (1:1, 2:1, 3:1, 4:1, 5:1, 6:1), dispersant concentrations (2.5, 3, 3.5, 4 and 4.5 wt%) and solid load (30, 35, 40, 45, 50 and 52 vol%), twenty-three experimental groups were evaluated, as summarized in Table 1.

Table 1: Different experimental groups with different dispersants, dispersant concentrations and solid load.

Nobel	Dispersant	Ratio	Dispersant concentration (wt%)	Solid load (vol%)
1#	CPD-03	- -	3	45
2#	CPD-03+CPD-05	1:1	3	45
3#	CPD-03+CPD-05	2:1	3	45
4#	CPD-03+CPD-05	3:1	3	45
5#	CPD-03+CPD-05	4:1	3	45
6#	CPD-03+CPD-05	5:1	3	45
7#	CPD-03+CPD-05	6:1	3	45
8#	CPD-03+CPD-05	4:1	2.5	45
9#	CPD-03+CPD-05	4:1	3	45
10#	CPD-03+CPD-05	4:1	3.5	45
11#	CPD-03+CPD-05	4:1	4	45
12#	CPD-03+CPD-05	4:1	4.5	45
13#	CPD-03+CPD-05	5:1	2.5	45
14#	CPD-03+CPD-05	5:1	3	45

Nobel	Dispersant	Ratio	Dispersant concentration (wt%)	Solid load (vol%)
15#	CPD-03+CPD-05	5:1	3.5	45
16#	CPD-03+CPD-05	5:1	4	45
17#	CPD-03+CPD-05	5:1	4.5	45
18#	CPD-03+CPD-05	5:1	3	30
19#	CPD-03+CPD-05	5:1	3	35
20#	CPD-03+CPD-05	5:1	3	40
21#	CPD-03+CPD-05	5:1	3	45
22#	CPD-03+CPD-05	5:1	3	50
23#	CPD-03+CPD-05	5:1	3	52

(3) Mould manufacturing and debinding

The silicon carbide mould was printed on a DLP printer (CeramPlus DLP-Flex, Zhejiang Jiaxing CeramPlus Tech. Ltd., China). The model file was imported into the printer by the relevant software, and then the required resin mould was printed with adjustment of the appropriate printing parameters. Compared with the traditional mould, the DLP mould has the advantages of convenient and quick fabrication; it is also easier to fabricate the mould with complex structures.

The SiC slurry was defoamed under vacuum for 5 minutes, then the obtained homogeneous slurry was poured into the DLP mould. After the mould had been filled, the mould was placed into an oven, heated to 80 °C and cured for 0.5 h to obtain SiC green bodies. In order to avoid cracking or collapse of the sample caused by the quick decomposition of the resin mould, the heating rate for debinding should be kept as slow as possible. Fig. 1 shows the thermogravimetric curve (TG, NETZSCH-Gerätebau GmbH, Germany) for the resin mould under nitrogen atmosphere. The decomposition rate of the mould is slow before 200 °C, before accelerating in the 200 – 400 °C range until the decomposition is complete at 600 °C. The following debinding and sintering profiles were used in a nitrogen-hydrogen mixture atmosphere: various heating rates of 1 K/min, 0.25 K/min and 0.5 K/min were implemented for the temperature range of RT – 200 °C, 200 – 400 °C, 400 – 600 °C and to keep the temperature at 600 °C for 2 h. To endow the sample with a certain strength after debinding, the temperature was finally increased to 1 250 °C at a heating rate of 2 K/min, and the temperature was kept for 2 h. Then the samples were naturally cooled to room temperature.

After debinding and burn-out of the mould, the SiC green bodies were heated to 2 100 °C under argon atmosphere and held for 2 h to obtain the final sintered ceramics.

(4) Characterization methods

The rheological behaviour of the different SiC suspensions was characterized by varying the shear rate from 1 to 100 s^{-1} at 25 °C with a Kinexus pro+ cone-plate toolkit with a diameter of 40 mm (Malvern, England). A Zetasizer Nano ZS (Malvern, England) was used to measure the particle size distribution in the suspensions. Sedimentation experiments were conducted with 45 vol% suspension to evaluate the effect of different proportions of dispersant on the stability of the suspension. The suspensions were kept and observed in 10-ml cylinders. After deposition for a period of time, the height of the sediment was recorded. The interference was observed for 480 h, and data were recorded every 12 h to evaluate the stability. The density of samples was measured with the Archimedes method (Sartorius, Germany). The flexural strength was tested with a three-point bending tester (SUN500, Cardano al Campo, Italy). The fracture surface of the samples was investigated with a scanning electronic microscope (SEM, Phenom Pro, Phenom World, Netherlands). The phase composition of the SiC raw powder and sintered samples was examined by means of X-ray diffraction (XRD, TD-3500, Tongda, China).

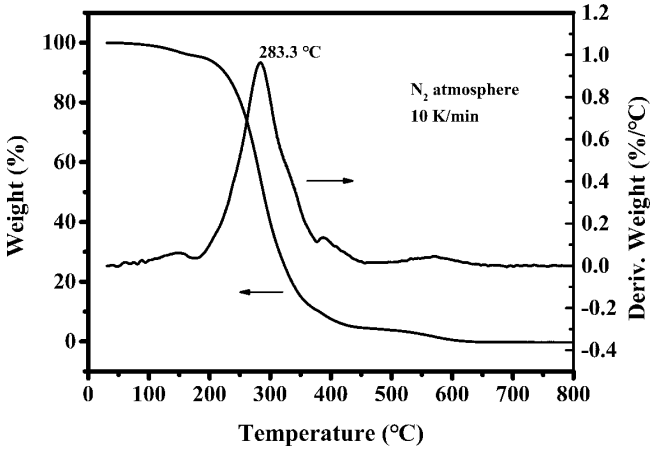

Fig. 1: Thermogravimetric curve of the resin mould.

III. Results and Discussions

(1) Effects of different dispersant types and dispersant ratios

A SiC ceramic suspension with high fluidity that can be generally obtained by using multiple dispersants at once is necessary for the densification of SiC ceramics during the forming processes and even the subsequent sintering processes. Adding a mix of dispersant can improve the dispersion effect of the powder [22]. Therefore, ratios of the CPD-03 and CPD-05 were selected as two components of

dispersant for the SiC suspension and discussed, the solid load being 45 vol% and dispersant content 3 wt%. As shown in Fig. 2 (a, b), compared with the suspension with only CPD-03 added, when two dispersants (CPD-03 and CPD-05) are combined, a suspension with lower viscosity can be obtained when the CPD-03 is the main component of the dispersant and a suspension with higher viscosity can be obtained when the CPD-05 is the main component of the dispersant. In addition, the viscosity of suspension with only CPD-03 added as dispersant increased sharply at a shear rate of 40 s^{-1} owing to an excessive disturbance of particles under the action of external forces caused by the irregular shape of the powder particles and poor absorption of dispersant on the particles' surface. So, the CPD-03 plays a dispersive role and a limited amount of the CPD-05 can further improve the dispersion of SiC particles and eliminate the shear thickening phenomenon. Finally, as shown in Fig. 2(c,d), a SiC suspension with a relatively low viscosity of 2.22 Pa·s and 2.20 Pa·s at a shear rate of 10 s^{-1} can be achieved when the ratio of CPD-03 and CPD-05 are 4:1 and 5:1, respectively, which is quite acceptable for the sample-forming process.

(2) Effects of dispersant concentrations

The rheological behaviour curves of different dispersant concentrations are shown in Fig. 3, with the ratio of CPD-03 to CPD-05 being 5:1. As shown in Fig. 3a, a suspension with the optimum viscosity can be achieved when the dispersant content is 3 wt%. For comparison, the viscosity at a shear rate of 10 s^{-1} of the suspensions formulated with different dispersant concentrations are shown in Fig. 3b. The viscosity decreased gradually from 2.62 Pa · s to 2.20 Pa · s with the concentration of dispersant increasing from 2.5 wt% to 3 wt%, whereas it increased from 2.20 Pa · s to 4.22 Pa · s with the concentration increasing from 3 wt% to 4.5 wt%. Therefore, 3 wt% dispersant concentration can be optimal to reduce the viscosity of SiC slurry. When the content of dispersant is less than 3 wt%, the surface of the SiC particles is not fully covered by the molecule, which leads to the high viscosity of suspension. When the content of dispersant is higher than 3 wt%, the amount of dispersant on the surface of SiC particles is oversaturated, which can potentially induce tangling between organic molecules, thus leading to flocculation, and thereby increasing the viscosity of the suspension. Fig. 3c shows the shear stress of the SiC slurry with different dispersant content. As the shear rate increased, the shear stress increased gradually. The effects of the rheological behaviour of the suspension can be described with the Herschel-Bulkley model [23]:

$$\tau = \tau_0 + K\gamma^n \quad (1)$$

where τ is the shear stress of the SiC suspension, τ_o is the yield stress of the SiC suspension, K is the consistency index, n is the flow behaviour index and γ is the shear rate. Model parameters are obtained with the fitting method using K and n.

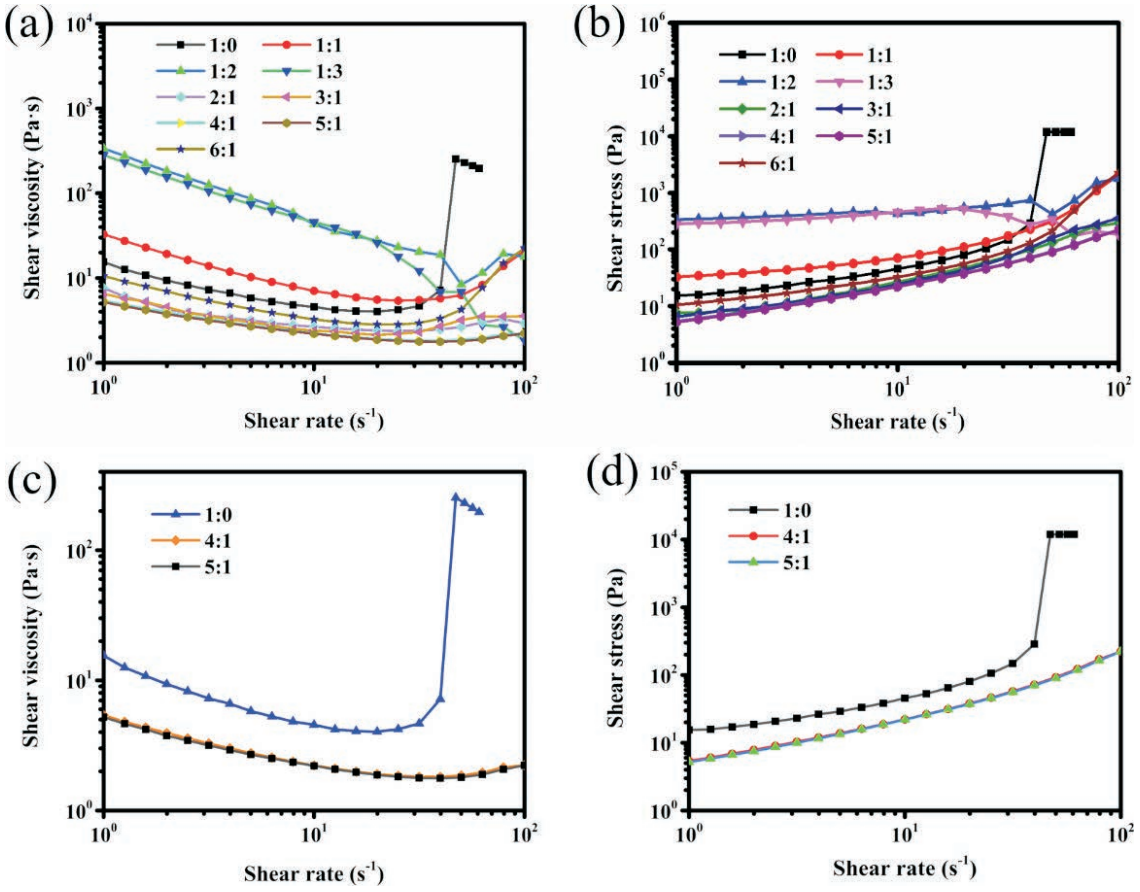

Fig. 2: (a) Viscosity-shear rate curves of SiC suspensions with various CPD-03:CPD-05 ratio, (b) shear stress-shear rate curves of SiC suspensions with various CPD-03:CPD-05 ratio, (c) viscosity-shear rate curves of the dispersants CPD-03 and CPD-05 is 4:1 and 5:1, (d) shear stress-shear rate curves of the proportions of dispersants CPD-03 and CPD-05 is 4:1 and 5:1. (solid load: 45 vol%).

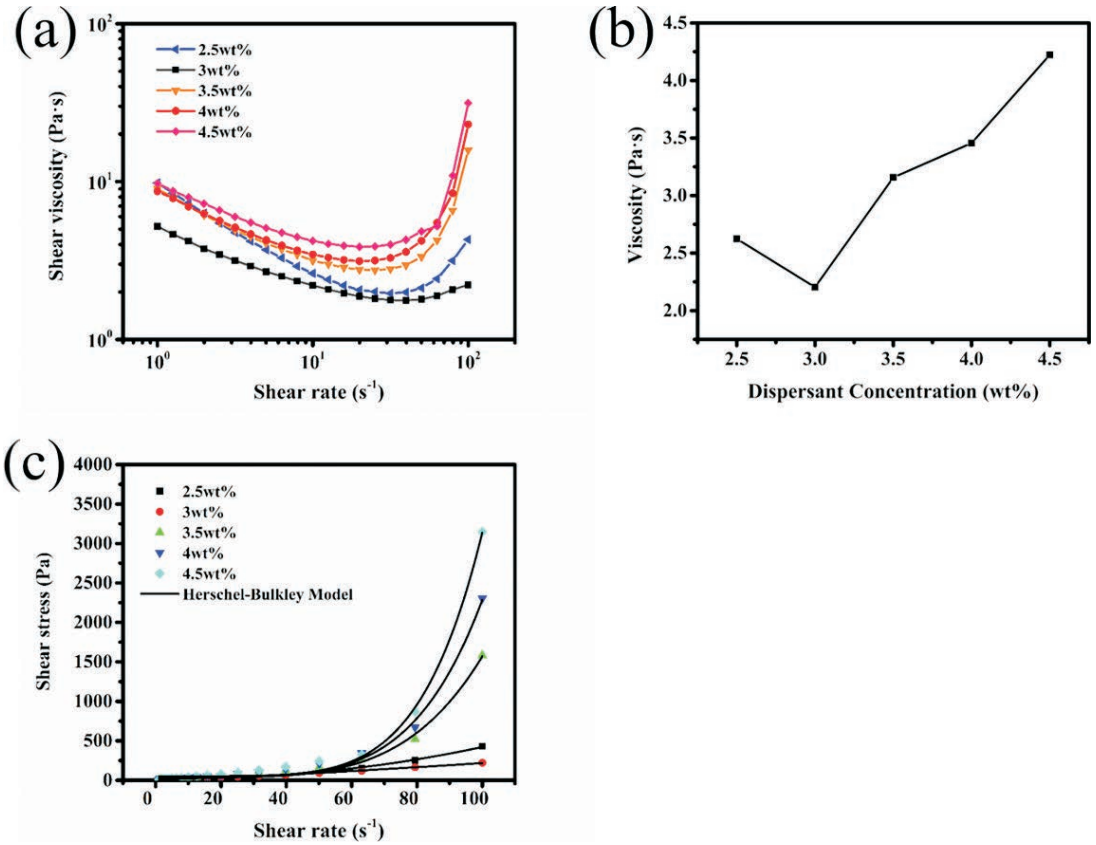

Fig. 3: (a) Viscosity-shear rate curves of SiC suspensions with different dispersants concentrations, (b) viscosity with different dispersants concentrations at a shear rate of 10 s^{-1}, (c) shear stress-shear rate curves of SiC suspensions with different dispersant concentrations, and the solid lines represent the Herschel-Bulkley model fitted. (the ratio of dispersant is 5:1; solid load: 45 vol%).

Differences between non-Newtonian fluid and Newtonian fluid were clearly characterized by the fluid characteristic constant n. The difference between n and 1 can be used as a non-Newtonian measure of fluid. The closer the n value to 1, the suspension tends to be a Newtonian fluid. And the smaller the k value, a suspension with lower viscosity can be achieved. Table 2 presents the fitting parameters, the R^2 was above 0.99, indicating a higher degree of fitting. The minimum τ_0 value (8.2766 Pa) and K value (0.5399) were achieved at 3 wt%, which is consistent with the previous viscosity shown in Fig. 3a.

Table 2: Effects of dispersant concentrations on Herschel-Bulkley model parameters of SiC suspensions (the ratio of dispersant is 5:1; solid load: 45 vol%).

Dispersant concentrations	τ_0	K	n	R^2
2.5	19.3398	1.0156	2.2058	0.9935
3	8.2766	0.5399	1.2955	0.9975
3.5	36.0476	1.8593	4.4582	0.9910
4	43.7256	2.7820	4.9531	0.9912
4.5	52.8671	3.2305	5.4901	0.9945

The rheological behaviour curves of various slurries with different dispersant concentrations with CPD-03: CPD-05 ratio fixed at 4:1 are shown in Fig. 4. As shown in Fig. 4a, the rheological curve behaviour was similar to that in Fig. 3a. When the content of dispersant was 3 wt%, the rheological behaviour was optimal. The viscosity of SiC suspensions with different dispersant concentrations at a shear rate of 10 s^{-1} decreases gradually from 2.74 Pa · s to 2.22 Pa · s with the concentration increasing from 2.5 wt% to 3 wt%, whereas it increases gradually from 2.22 Pa · s to 3.87 Pa · s with the concentration increasing from 3 wt% to 4.5 wt%. Compared with the results of the rheological curves in Fig. 4, the rheological behaviour of SiC suspensions is also different when different proportions of dispersants are used. From Table 3, when the content of dispersant was 3 wt%, it was found that the K was 0.6287, which is larger than the K (0.5399) of the suspension when the dispersant ratio is 5:1. So, when the ratio of dispersants is 5:1 and the content of dispersant is 3 wt%, the SiC suspension exhibits optimum rheological behaviour.

Table 3: Effects of dispersant concentrations on Herschel-Bulkley model parameters of SiC suspensions (the ratio of dispersant is 4:1; solid load: 45 vol%).

Dispersant concentration	τ_0	K	n	R^2
2.5	34.8286	2.1465	7.5627	0.9945
3	7.9729	0.6287	1.2655	0.9982
3.5	8.8775	1.1982	1.1494	0.9958
4	10.4302	0.6323	1.3746	0.9988
4.5	50.9860	1.9742	7.5276	0.9755

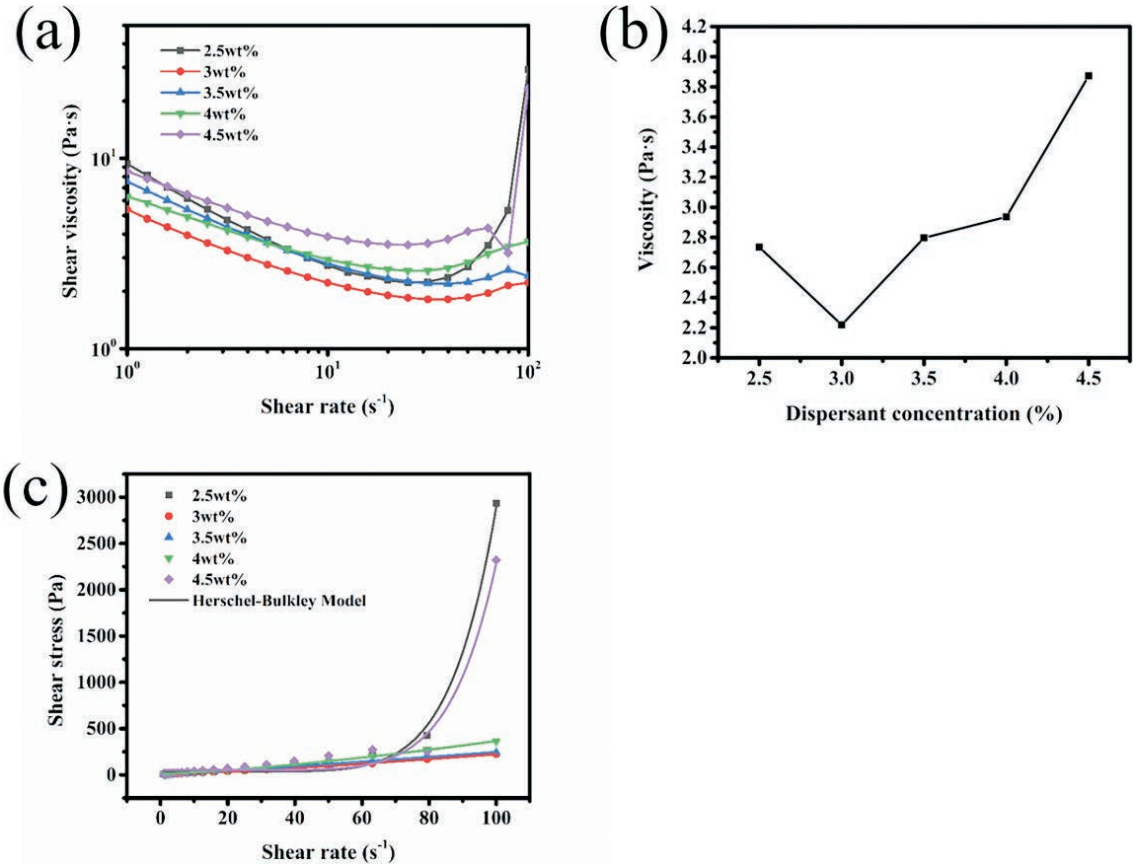

Fig. 4: (a) Viscosity-shear rate curves of SiC suspensions with different dispersants concentrations, (b) viscosity with different dispersants concentrations at a shear rate of 10 s^{-1}, (c) shear stress-shear rate curves of SiC suspensions with different dispersant concentrations, and the solid lines represent the Herschel-Bulkley model fitted. (the ratio of dispersant is 4:1; solid load: 45 vol%).

(3) Suspension stability

The particle size distribution of the SiC suspensions with different dispersant ratios was also measured. Fig. 5 shows the distribution of SiC particles in a 40-vol% solid-loading suspension. Even though d_{50} of both the true particles is 458.7 nm, a small amount of particle agglomeration resulted when the ratio of the dispersants was 4:1. It can affect the properties of sintered samples. Therefore, based on the above experimental research, when the ratio of dispersant CPD-03 to CPD-05 is 5:1, the dispersion and stability of SiC suspension are optimal.

A sedimentation test was conducted to gauge the influence of the dispersants on the stability of the suspension system. As shown in Fig. 6, the relationship between the sedimentation height (supernate) and the initial height was recorded after 480 h, and the stability of the SiC suspension was evaluated. The optimum sedimentation volume ratio of 99.4 % was achieved at a ratio between CPD-03 and CPD-05 of 5:1.

In addition to the dispersant that affects the dispersion of the slurry, the oxygen content in the SiC powder also has a significant effect on dispersity [24–25], but the oxygen content in the study is basically unchanged, so it has not been systematically discussed.

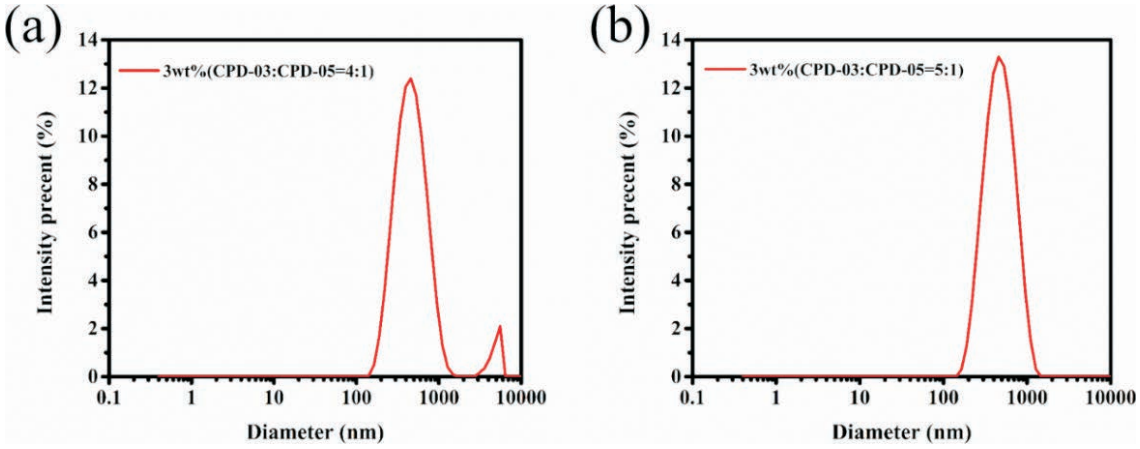

Fig. 5: (a) Particle size distribution in 40 vol% suspensions with the ratio of dispersant is 4:1, (b) particle size distribution in 40 vol% suspensions with the ratio of dispersant is 5:1.

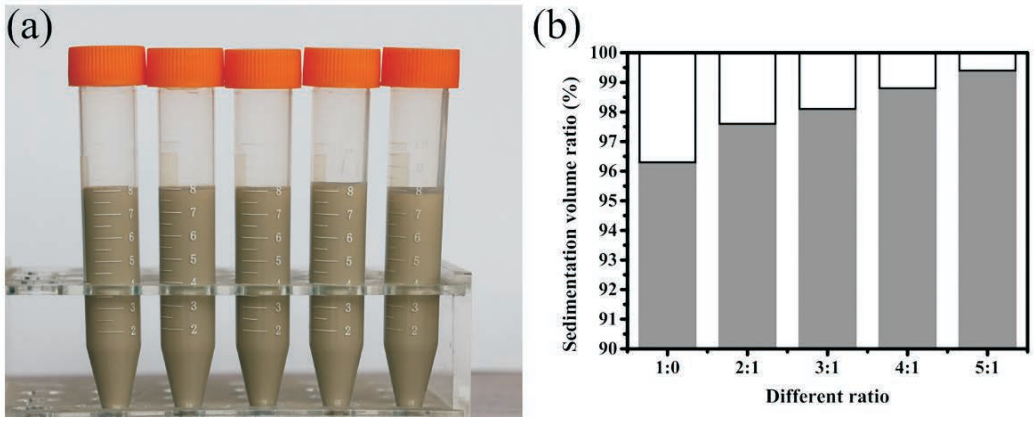

Fig. 6: (a) SiC suspensions with different dispersant ratios after 480 h settling, (b) sedimentation volume ratio of SiC with different proportion of dispersant CPD-03 and CPD-05. (solid load: 45 vol%; dispersant concentration: 3 wt%).

(4) Effects of the solid load

In order to fabricate SiC ceramic devices with high density, it is necessary to meet the requirements for a high solid load in the SiC suspension. Based on the above experimental results, the effect of the solid load on the rheological behaviour of SiC suspension was studied based on the selection of CPD-03 and CPD-05 at a ratio of 5:1 and a concentration of 3 wt%. Fig. 7 shows that the viscosity of the SiC suspension is closely related to the solid load; with the increase in the solid load, the viscosity increases. When the solid load is lower than 50 vol%, the suspension system is relatively stable with better dispersion and lower viscosity. When the solid load is 50 vol%, the viscosity of the suspension is 2.78 Pa·s at a shear rate of 40 s^{-1}, which is still a low value. When the solid load is 52 vol%, the rheological behaviour of the SiC suspension changes considerably. When the shear rate is higher than 25 s^{-1}, the suspension begins to undergo intense shear thickening, which indicates the dispersion ability of the dispersant to reach nearly the maximum. Because the particle distribution space becomes smaller with the increase of the solid load, frequent collisions and friction occur between particles, which makes the viscosity increase rapidly. When the shear rate is higher than 36 s^{-1}, the viscosity of the suspension decreases with the increase in the shear rate. After this shear-thickening region, the viscosity can neither become so great that fracture of the sample occurs nor can the viscosity level out to a new plateau value. In some specific situations, the viscosity has been seen to decrease yet again after this Newtonian region [26]. According to Fig. 7c, with the increase in the solid load, the shear stress becomes dramatically higher. The fitting parameters are given in Table 4. The R^2 values were over 0.99, revealing that the experiment data were fitted well to the Herschel-Bulkley model. According to the obtained results, with the increase in solid load from 30 vol% to 50 vol% (owing to the special type of fluid with 52 vol% solid load, the rheological curve cannot be fitted correctly and reasonably with the model), K and τ_0 increased from 0.3566 to 0.4265 and 1.3739 to 22.0589, respectively. It suggests that the viscosity increased with the increased solid load, which shows no difference to the results in Fig. 7a. As shown in Fig. 7b, when the shear rate is 10 s^{-1}, with the solid load increase from 30 vol% to 52 vol%, the viscosity increases gradually from 0.54 Pa·s to 6.82 Pa·s, the viscosity increases significantly as the solid load increases from 45 vol% to 52 vol%. Indeed, the shear viscosity increases with the increase in the SiC solid load and sharply with high solid loads. Different models have been formulated to describe the relationship between the solid load and viscosity [27–29]. The Krieger-Dougherty model provides a good estimation of the suspensions' behaviours:

$$\eta_r = \frac{\eta_s}{\eta_d} = (1 - \frac{\phi}{\phi_m})^{-B\phi_m} \quad (2)$$

where B is the Einstein coefficient, η_r is the relative viscosity between the suspension (η_s) and dispersion medium (η_d). This relationship is a popular choice for fitting to experimental data, in which case B and ϕ_m are considered to be fitting parameters. The fitting parameter ϕ_m is 56.01. The results show that the theoretical maximum solid load can reach 56.01 vol% in the system.

Table 4: Effects of the solid load on Herschel-Bulkley model parameters of SiC suspensions (dispersant concentration: 3 wt%).

Solid load	τ_0	K	n	R^2
30	1.3739	0.3566	1.0220	0.9993
35	3.6729	0.2963	1.2610	0.9978
40	9.4335	0.1077	1.6441	0.9937
45	8.2766	0.5399	1.2955	0.9975
50	22.0589	0.4265	1.4525	0.9951
52	--	--	--	--

With the increase in the solid load, the volume occupied by resin in the suspension is reduced commensurately. So that the space left for the SiC particles to move is too small to maintain Brownian motion, the interaction between the powder particles is increased significantly, which makes it difficult for the SiC particles to move and leads to an increase in viscosity.

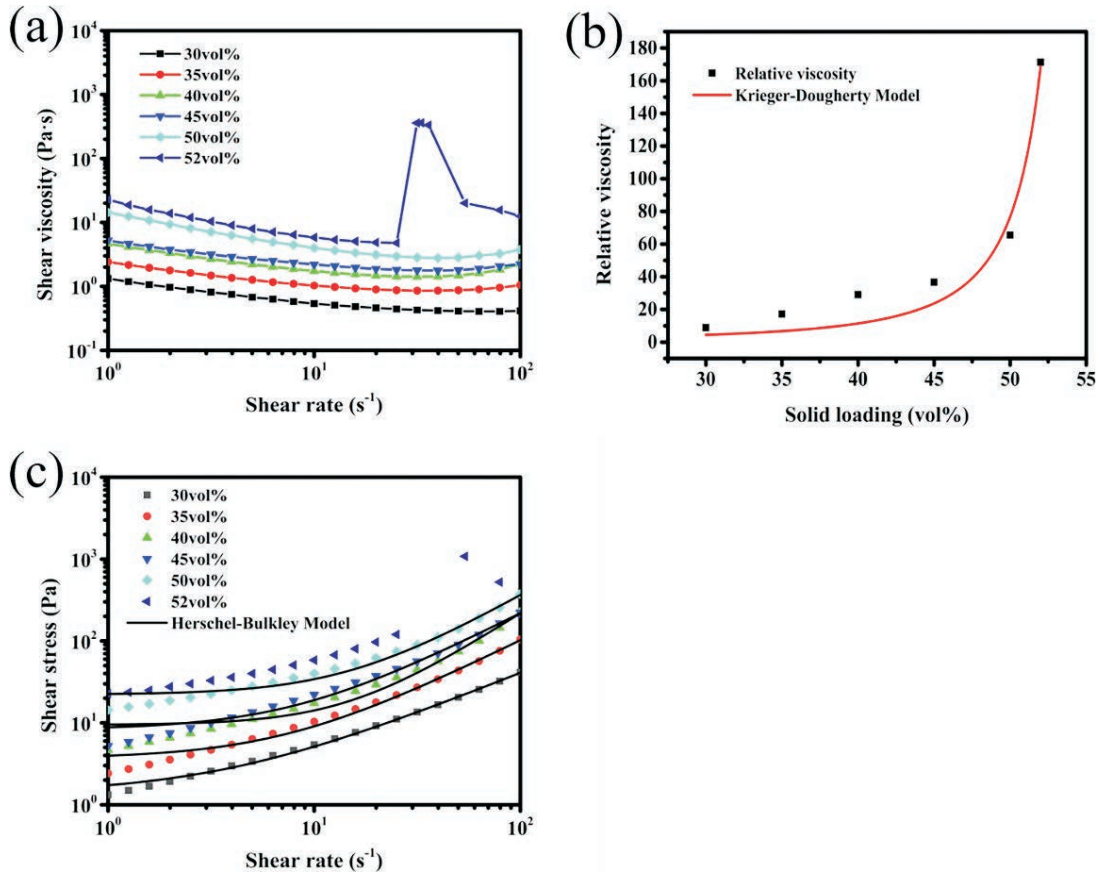

Fig. 7: (a) Viscosity-shear rate curves of SiC suspensions with different solid-load, (b) relative viscosity of dependence on dispersant concentration at a shear rate of 10 s^{-1}, and the solid line adjustment to the Krieger-Dougherty Model, (c) shear stress-shear rate curves of SiC suspensions with different solid-load, and the solid lines represent the Herschel-Bulkley Model fitted (solid-load: 30 vol% – 50 vol%). (dispersant concentration: 3 wt%).

(5) Mechanical properties

The mechanical properties of sintered samples prepared with different SiC suspensions with varying dispersant ratios were investigated. The SiC ceramic samples measured 35 mm × 4 mm × 3 mm in size. For each flexural test result, > 5 samples were tested. The relative density and flexural strength of different sintered samples are shown in Fig. 8. For SiC ceramic samples prepared from different suspensions with dispersant CPD-03 to CPD-05 ratio at 1:0, 3:1, 4:1, 5:1, the relative density and flexural strength measured 87.31 %, 90.82 %, 92.81 %, 95.16 % and 206.4 MPa, 255.8 MPa, 326.7 MPa, 377.4 MPa, respectively. Fig. 9 abcd shows the microstructure of the sintered samples with various CPD-03 : CPD-05 ratios. It can be seen that the phenomenon of non-homogeneous distribution of the second phase gradually disappears with the increase in the dispersant ratio. As can be seen from Fig. 9ab, the non-homogeneous distribution of the second phase is more serious, so the number of long-column crystals is greater, and the small pores can be easily adsorbed in the non-homogeneous distribution, which is not conducive to the strength of the sintered samples. From Fig. 9cd it can be seen that with the weakening of the uneven distribution of the second phase, the grains gradually grow into fine equiaxed grains, and the strength increases. However, the density of B_4C is lower than that of SiC, so although the sintering is dense, as can be seen from Fig. 9d, the relative density of the final sintered sample only reaches 95.16 %. The results show that the densification and strength of the sintered samples are optimum when the suspension exhibits excellent rheological behaviour. As shown in Fig. 10, the density and mechanical properties of SiC sintered samples prepared in the gel casting process are better than those previous reported [30–36]. However, Zhang *et al.* prepared SiC slurry with solid load of 52 vol% and additionally used dextrin as a carbon source, and the highest mechanical properties of sintered samples reached 531 MPa. Therefore, in our future study, the aim is to further improve the solid load in SiC ceramics.

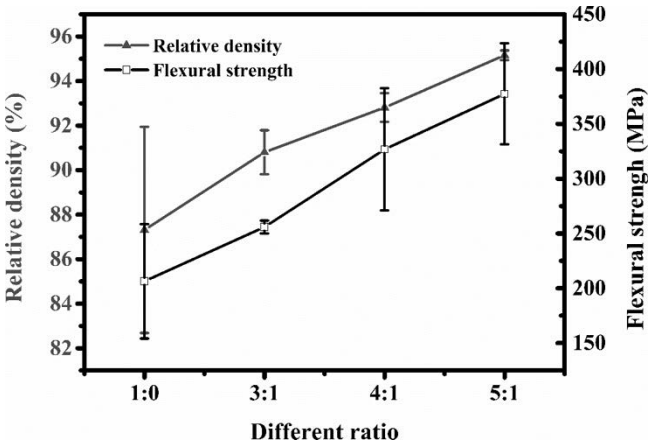

Fig. 8: Effects of dispersant ratios on the relative density and flexural strength of SiC samples.

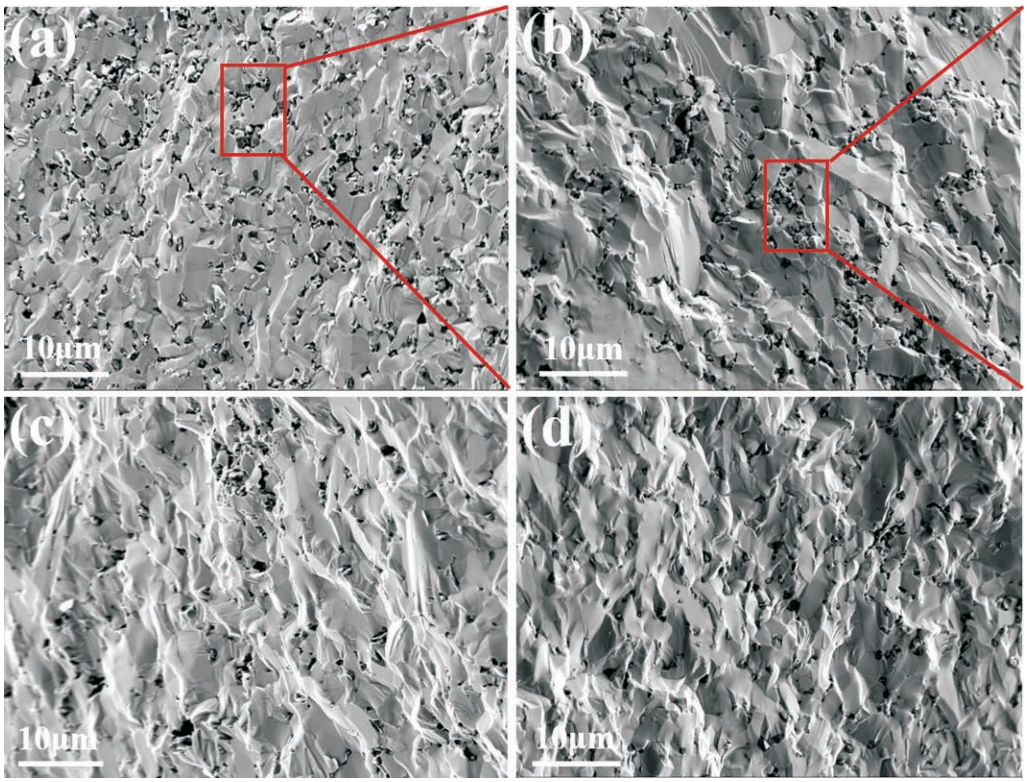

Fig. 9: Microstructure image of the sintered SiC ceramic with the fracture surface: (a) 1:0; (b) 3:1; (c) 4:1; (d) 5:1.

Fig. 11 shows XRD spectra of SiC raw powders and sintered samples with different dispersant ratios. The phase of the SiC raw powders and sintered samples are β-and α-SiC phase, respectively, and the β-SiC has been completely transformed into α-SiC on completion of sintering. Furthermore, the XRD diffraction peaks of the sintered SiC samples have obviously been shifted to the high angle as a result of the addition of the boron carbide. During the sintering process, the B replaces the Si, and the lattice constant decreases because the radius of B is smaller than that of Si, which makes the peak shift to the right [3,37–38]. Uniformly dispersed boron carbide can lead to homogeneous diffusion in silicon carbide, thus increasing the number of lattice defects, accelerating the growth of fine equiaxed crystals and promoting sintering.

The SiC test bar for flexural strength testing and a honeycomb structure were prepared with the gel casting method based on the optimal SiC slurry formula with a solid load of 45 vol% as shown in Fig. 12. The sintered ceramic samples have no obvious defects or large cracks. As shown in Fig. 12a, there is no significant difference between the SiC test bar and the standard pattern. Fig. 12b shows the honeycomb structure with a wall thickness of 0.7 mm and a true density of 2.98 g/cm^3. There are some small pores and defects on the surface of the sample owing to the heat curing reaction, which is also a problem that we need to resolve in our future research.

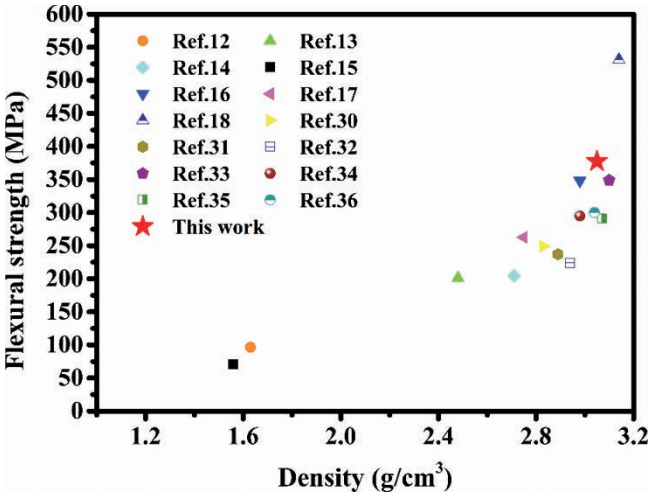

Fig. 10: Comparison of flexural strength of silicon carbide complex structures with previous reported.

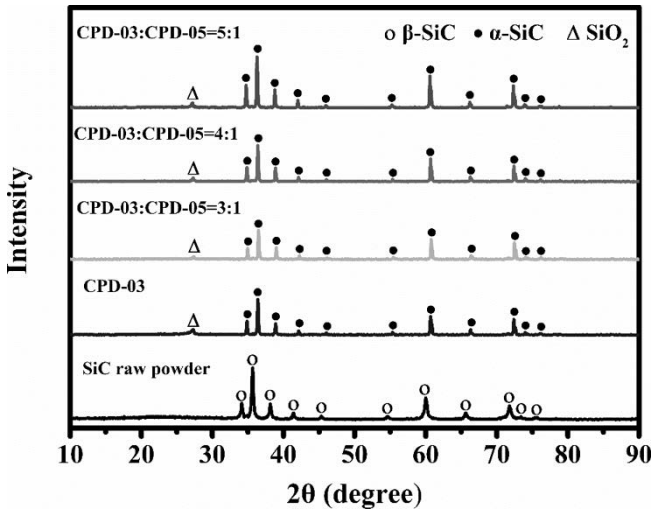

Fig. 11: XRD spectra of SiC raw powders and sintered samples with different dispersant ratio.

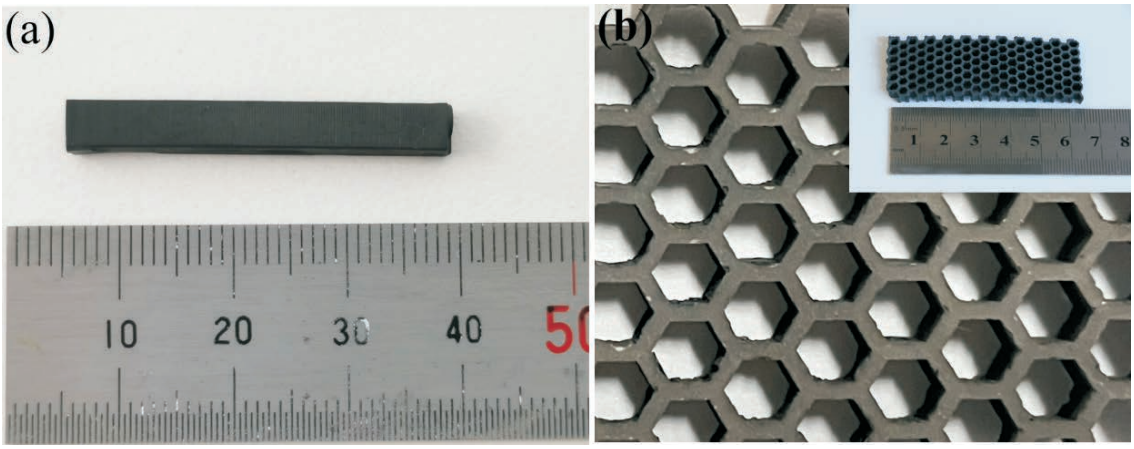

Fig. 12: The gel casting of SiC ceramic with test bar and honeycomb structures.

V. Conclusions

In this work, the effect of dispersant types, dispersant concentrations and solid load on the dispersion behaviour, rheological behaviour and stability of the SiC suspensions was discussed in detail. Appropriate dispersant can increase dispersion and reduce the viscosity of the suspensions. Furthermore, a SiC suspension with better rheological behaviour can be obtained by adding dispersants mixed with various components. The rheological behaviour of the SiC suspension is optimal when the proportion of dispersant is 5:1, the minimum viscosity is 2.20 Pa · s and the shear rate is 10 s^{-1}. The SiC suspension with 45 vol% solid load was prepared based on this formulation. SiC ceramic green bodies were prepared with the gel casting method without obvious cracks. SiC ceramic with 377.4 MPa flexural strength with 95.16 % relative density was obtained after sintering. This forms a cornerstone for the fabrication of SiC ceramics with a complex structure and acceptable mechanical performance.

Acknowledgments

This work has been supported by the National Key R&D Program of China (2017YFB1103500 & No. 2017YFB1103502).

References

1 Yuan, S., Yang, Z., Chen, G.: 3D microstructure model and thermal shock failure mechanism of a Si_3N_4-bonded SiC ceramic refractory with SiC high volume ratio particles, *Ceram. Int.,* **45** [4], 4219 – 4229, (2019).

2 Rodríguez-Rojas, F., Ortiz, A.L., Guiberteau, F., Nygren, M.: Anomalous oxidation behaviour of pressureless liquid-phase-sintered SiC, *J. Eur. Ceram. Soc.,* **31** [13], 2393 – 2400, (2011).

3 Liu, J., Tian, C., Xiao, H., Guo, W., Gao, P., Liang, J.: Effect of B_4C on co-sintering of SiC ceramic membrane, *Ceram. Int.,* **45** [3], 3921 – 3929, (2019).

4 Padture, N.P.: Advanced structural ceramics in aerospace propulsion, *Nat. Mater.*, **15** [8], 804 – 809, (2016).

5 Katoh, Y., Snead, L.L., Szlufarska, I., Weber, W.J.: Radiation effects in SiC for nuclear structural applications, *Curr. Opin. Solid State Mater. Sci.*, **16** [3], 143 – 152, (2012).

6 Khorrami, M.S., Kazeminezhad, M., Miyashita, Y., Saito, N., Kokabi, A.H.: Influence of ambient and cryogenic temperature on friction stir processing of severely deformed aluminum with SiC nanoparticles, *J. Alloy. Compd.*, **718**, 361 – 372, (2017).

7 Hurst, J.B., Dutta, S.: Simple processing method for high-strength silicon carbide, *J. Am. Ceram. Soc.*, **70** [11], 303 – 308, (1987).

8 Reiterer, M., Kraft, T., Janosovits, U., Riedel, H.: Finite element simulation of cold isostatic pressing and sintering of SiC components, *Ceram. Int.*, **30** [2], 177 – 183, (2004).

9 Suzuki, T.S., Uchikoshi, T., Sakka, Y.: Effect of sintering conditions on microstructure orientation in α-SiC prepared by slip casting in a strong magnetic field, *J. Eur. Ceram. Soc.*, **30** [14], 2813 – 2817, (2010).

10 Yang, S., Zhang, R., Qu, X.: X-ray analysis of powder-binder separation during SiC injection process in L-shaped mould, *J. Eur. Ceram. Soc.*, **35** [1], 61 – 67, (2015).

11 Badini, C., Fino, P., Ortona, A., Amelio, C.: High temperature oxidation of multilayered SiC processed by tape casting and sintering, *J. Eur. Ceram. Soc.*, **22** [12], 2071 – 2079, (2002).

12 Compton, B.G., Lewis, J.A.: 3D-printing of lightweight cellular composites, *Adv. Mater.*, **26** [34], 5930 – 5935, (2014).

13 Jin, L., Zhang, K., Xu, T., Zeng, T., Cheng, S.: The fabrication and mechanical properties of SiC/SiC composites prepared by SLS combined with PIP, *Ceram. Int.*, **44** [17], 20992 – 20999, (2018).

14 He, R., Ding, G., Zhang, K., Li, Y., Fang, D.: Fabrication of SiC ceramic architectures using stereolithography combined with precursor infiltration and pyrolysis, *Ceram. Int.*, **45** [11], 14006 – 14014, (2019).

15 Larson, C.M., Choi, J.J., Gallardo, P.A., Henderson, S.W., Niemack, M.D.: Direct ink writing of silicon carbide for microwave Optics: direct ink writing of silicon carbide for microwave, *Adv. Eng. Mater.*, **18** [1], 39 – 45, (2016).

16 Liu, K., Wu, T., Bourell, D.L., Tan, Y., Wang, J.: Laser additive manufacturing and homogeneous densification of complicated shape SiC ceramic parts, *Ceram. Int.*, **44** [17], 21067 – 21075, (2018).

17 Zhang, H., Yang, Y., Hu, K., Liu, B., Liu, M., Huang, Z.: Stereolithography-based additive manufacturing of lightweight and high-strength C_f/SiC ceramics, *Addit. Manuf.*, **34**, 101199, (2020).

18 Zhang, J., Jiang, D., Lin, Q., Chen, Z., Huang, Z.: Properties of silicon carbide ceramics from gelcasting and pressureless sintering, *Mater. Des.* **65**, 12 – 16, (2015).

19 Tu, T., Jiang, G.: SiC reticulated porous ceramics by 3D printing, gelcasting and liquid drying, *Ceram. Int.*, **44** [3], 3400 – 3405, (2018).

20 Chen, F., Liu, K., Sun, H., Shui, Z., Liu, C., Chen, J., Shi, Y.: Fabrication of complicated silicon carbide ceramic components using combined 3D printing with gelcasting, *Ceram. Int.*, **44** [1], 254 – 260, (2018).

[21] Zhang, S., Sha, N., Zhao, Z.: Surface modification of α-Al_2O_3 with dicarboxylic acids for the preparation of UV-curable ceramic suspensions, *J. Eur. Ceram. Soc.*, **37** [4], 1607 – 1616, (2017).

[22] Richard, E.M., Eric, R.T.: *Tape Casting: Theory and Practice*. Wiley-American Ceramic Society, 2000.

[23] Herschel, V.W.H., Bulkley, R.: Consistency measurements of rubber-benzene solutions, (in German), *Kolloid Z.*, **39**, 291 – 300, (1926).

[24] Zhou, L., Huang, Y., Xu, X., Xie, Z., Yang, J., Ma, L.: Influence of oxygen content on IEP and dispersity of silicon carbide powder, *High, Tech. Lett*., 2000.

[25] Feng, D., Ren, Q., Ru, H., Wang, W., Jiang, Y., Ren, S., Zhang, C.: Effect of oxygen content on the sintering behaviour and mechanical properties of SiC ceramics, *Ceram. Int*., **45** [18], 23984 – 23992, (2019).

[26] Barnes, H.A.: Shear thickening ("Dilatancy") in suspensions of nonaggregating solid particles dispersed in newtonian liquids, *J. Rheol.*, **33** [2], 329 – 366, (1989).

[27] Krieger, I.M., Dougherty, T.J.: A mechanism for non-newtonian flow in suspensions of rigid spheres, *Trans. Soc. Rheol.*, **3** [1], 137 – 152, (1959).

[28] Mueller, S., Llewellin, E.W., Mader, H.M.: The rheology of suspensions of solid particles, *Proc. R. Soc. Math. Phys. Eng. Sci.*, **466** [2116], 1201 – 1228, (2010).

[29] Liu, D.-M.: Particle packing and rheological property of highly-concentrated ceramic Suspensions: Φ_m determination and viscosity prediction, *J. Mater. Sci.*, **35**, 5503 – 5507, (2000).

[30] Zhu, W., Fu, H., Xu, Z., Liu, R., Jiang, P., Shao, X., Shi, Y., Yan, C.: Fabrication and characterization of carbon fiber reinforced SiC ceramic matrix composites based on 3D printing technology, *J. Eur. Ceram. Soc.*, **38** [14], 4604 – 4613, (2018).

[31] Fu, H., Zhu, W., Xu, Z., Chen, P., Yan, C., Zhou, K., Shi, Y.: Effect of silicon addition on the microstructure, mechanical and thermal properties of C_f/SiC composite prepared via selective laser sintering, *J. Alloy. Compd.*, **792**, 1045 – 1053, (2019).

[32] Wahl, L., Lorenz, M., Biggemann, J., Travitzky, N.: Robocasting of reaction bonded silicon carbide structures, *J. Eur. Ceram. Soc.*, **39** [15], 4520 – 4526, (2019).

[33] Song, S., Lu, B., Gao, Z., Bao, C., Ma, Y.: Microstructural development and factors affecting the performance of a reaction-bonded silicon carbide composite, *Ceram. Int.*, **45**, [14], 17987 – 17995, (2019).

[34] Fallah-Arani, H., Isafi, S., Tabrizian, P., Siavash Moakhar, R., Baghshahi, S.: A novel gel-cast SiC with potential application in turbine hot section: investigation of the rheological behavior and mechanical properties, *Ceram. Int.*, **45** [13], 15996 – 16001, (2019).

[35] Xing, Y., Wu, H., Liu, X., Huang, Z.: Aqueous gelcasting of solid-state-sintered SiC ceramics with the addition of the copolymer of isobutylene and maleic anhydride, *J. Mater. Process. Technol.*, **271**, 172 – 177, (2019).

[36] Zhang, Y., Yuan, Z., Zhou, Y.: Gelcasting of silicon carbide ceramics using phenolic resin and furfuryl alcohol as the gel former, *Ceram. Int*., **40** [6], 7873 – 7878, (2014).

[37] Maddrell, E.R.: Pressureless sintering of silicon carbide, *J. Mater. Sci. Lett.*, **6** [4], 486 – 488, (1987).

[38] Ermer, E., Ptak, W.S.: FTIR studies of structural effects due to boron addition in sintered silicon carbide, *Vib. Spectrosc.*, **29** [2], 211 – 215, (2002).